

Clark University

Clark Digital Commons

---

Geography

Faculty Works by Department and/or School

---

5-2023

## Limited Evidence of Cumulative Effects From Recurrent Droughts in Vegetation Responses to Australia's Millennium Drought

Tong Jiao  
*Clark University*

Christopher A. Williams  
*Clark University, cwilliams@clarku.edu*

Martin De Kauwe  
*University of New South Wales*

Belinda E. Medlyn  
*Western Sydney University*

Follow this and additional works at: [https://commons.clarku.edu/faculty\\_geography](https://commons.clarku.edu/faculty_geography)



Part of the [Geography Commons](#)

---

### Repository Citation

Jiao, Tong; Williams, Christopher A.; De Kauwe, Martin; and Medlyn, Belinda E., "Limited Evidence of Cumulative Effects From Recurrent Droughts in Vegetation Responses to Australia's Millennium Drought" (2023). *Geography*. 944.

[https://commons.clarku.edu/faculty\\_geography/944](https://commons.clarku.edu/faculty_geography/944)

This Article is brought to you for free and open access by the Faculty Works by Department and/or School at Clark Digital Commons. It has been accepted for inclusion in Geography by an authorized administrator of Clark Digital Commons. For more information, please contact [larobinson@clarku.edu](mailto:larobinson@clarku.edu), [cstebbins@clarku.edu](mailto:cstebbins@clarku.edu).



## RESEARCH ARTICLE

10.1029/2022JG006818

### Key Points:

- Cumulative effects affected 8%–20% of fire-free landscape exposed to repeat or long-duration droughts during the Millennium Drought period
- Despite being relatively infrequent, cumulative effects doubled drought impacts in areas where they occurred
- Large effects in forests and savannas implies a greater risk of carbon release given recurrent drought events

### Supporting Information:

Supporting Information may be found in the online version of this article.

### Correspondence to:





C. A. Williams,  
cwilliams@clarku.edu

### Citation:

Jiao, T., Williams, C. A., De Kauwe, M. G., & Medlyn, B. E. (2023). Limited evidence of cumulative effects from recurrent droughts in vegetation responses to Australia's Millennium Drought. *Journal of Geophysical Research: Biogeosciences*, 128, e2022JG006818. <https://doi.org/10.1029/2022JG006818>

Received 22 JAN 2022  
Accepted 25 APR 2023

# Limited Evidence of Cumulative Effects From Recurrent Droughts in Vegetation Responses to Australia's Millennium Drought

Tong Jiao<sup>1</sup> , Christopher A. Williams<sup>1</sup> , Martin G. De Kauwe<sup>2,3,4,5</sup> , and Belinda E. Medlyn<sup>6</sup> 

<sup>1</sup>Graduate School of Geography, Clark University, Worcester, MA, USA, <sup>2</sup>ARC Centre of Excellence for Climate Extremes, Sydney, NSW, Australia, <sup>3</sup>Climate Change Research Centre, University of New South Wales, Sydney, NSW, Australia, <sup>4</sup>Evolution & Ecology Research Centre, University of New South Wales, Sydney, NSW, Australia, <sup>5</sup>School of Biological Sciences, University of Bristol, Bristol, UK, <sup>6</sup>Hawkesbury Institute for the Environment, Western Sydney University, Penrith, NSW, Australia

**Abstract** Drought-induced vegetation declines have been reported across the globe and may have widespread implications for ecosystem composition, structure, and functions. Thus, it is critical to maximizing our understanding of how vegetation has responded to recent drought extremes. To date, most drought assessments emphasized the importance of drought intensity for vegetation responses. However, drought timing, duration, and repeat exposure all may be important aspects of ecosystem response with the potential for non-linear effects. Cumulative effects are one such phenomenon, representing the additional decline due to repeated exposure to drought, and indicating gradual loss of ecosystem resistance. This study quantifies the frequency and magnitude of cumulative effects among Australian ecosystems as they responded to the Millennium Drought. Three distinct biophysical variables derived from satellite remote sensing were analyzed, including fraction of photosynthetically absorbed radiation, photosynthetic vegetation cover, and canopy density derived from passive microwave data. Cumulative effects were detected in only 8%–20% of the fire-free landscape exposed to repeat or long-duration drought, and could be a statistical artifact. In those limited cases, they approximately doubled drought impacts on leaf abundance, canopy cover, and vegetation density. Cultivated lands and grasslands were the most susceptible to cumulative effects, losing resistance to recurrent droughts, but could be false discovery. Despite being relatively infrequent in forests and savannas, cumulative effects caused larger additional declines in these ecosystems. Overall, our study demonstrates that repeated exposure appears to have limited influence on the magnitude of drought impacts on canopy structure affecting only a few areas.

## 1. Introduction

During the past few decades, reports of vegetation decline associated with drought have been on the rise across the globe (Allen et al., 2010), including in North America (D. D. Breshears et al., 2005), Europe (Ciais et al., 2005; Ivits et al., 2014; Reichstein et al., 2007), the Amazon basin (Phillips et al., 2009, 2010), Asia (Y Liu et al., 2014), and Australia (Fensham & Fairfax, 2007; Matusick et al., 2013; van Dijk et al., 2013). Extensive plant mortality has the potential to trigger abrupt and irreversible changes in ecosystem composition (Allen & Breshears, 1998; Suarez & Kitzberger, 2008), which would have profound implications for biodiversity, ecosystem function, ecosystem services, and land-climate interactions (Anderegg, Kane, & Anderegg, 2013; C. A. Williams et al., 2016). In addition, droughts can cause a substantial reduction of ecosystem productivity, reducing the capacity for plants to take up carbon from the atmosphere (Lewis et al., 2011; Schwalm et al., 2012) and contributing to positive carbon-climate feedbacks (Lindner et al., 2010). Given the forecast of future drought with increased intensity, frequency, duration as well as spatial extent under global warming (Dai, 2013; Held & Soden, 2006; Sheffield & Wood, 2008; Ukkola et al., 2020; C. A. Williams, 2014; I. N. Williams et al., 2014), it is critical to investigate vegetation response to recent drought as the basis of predicting future drought impacts and related consequences in carbon and water cycles.

Current studies of vegetation responses to extreme drought have mostly emphasized the importance of drought intensity (DI) in determining the magnitude of drought impact. At local scales, drought experiments and in situ investigation of recent extreme events indicate that abnormally low precipitation tends to suppress photosynthesis and increase mortality in forest ecosystems (Doughty et al., 2015; Keith et al., 2012; Nepstad et al., 2007;

© 2023. The Authors.

This is an open access article under the terms of the [Creative Commons Attribution-NonCommercial-NoDerivs License](https://creativecommons.org/licenses/by/4.0/), which permits use and distribution in any medium, provided the original work is properly cited, the use is non-commercial and no modifications or adaptations are made.

Phillips et al., 2009). For some species, there exists a threshold of DI beyond which extensive forest mortality will occur independent of tree density (Floyd et al., 2009). A hydraulic-based threshold of drought stress has been identified during the mortality of aspen in southwestern United States in early 2010s and it has hindcasted the regional pattern of tree mortality with reasonable accuracy when compared to field plots and mortality maps derived from Landsat imagery (Anderegg, Flint, et al., 2015). At broader spatial scales, ecosystem modeling simulated substantial decreases of primary productivity associated with severe drought (Craig et al., 2002; Y Liu et al., 2014; Reichstein et al., 2007; Schwalm et al., 2011). Based on satellite observations, large-scale drought assessments also demonstrate large negative anomalies in vegetation greenness, ecosystem productivity, as well as the length of growing season in response to large water deficit (D. D. Breshears et al., 2005; Ma et al., 2015; Schwalm et al., 2010, 2012). While biomes generally show resilience to modest interannual water variability, ecosystem resilience can be threatened by hydro-climatic extremes (Ponce-Campos et al., 2013).

Compared to DI, the temporal pattern of drought also plays a critical role in determining drought impacts. For instance, recurrent or long-duration droughts can induce additional vegetation decline in response to the same DI (Bigler et al., 2007; Mueller et al., 2005; Serra-Maluquer et al., 2018). Possible mechanisms underlying the cumulative drought effects include accumulated hydraulic deterioration caused by cavitation fatigue over successive droughts (Anderegg, Plavcová, et al., 2013), limited capacity of regeneration due to depleted non-structural carbohydrate reserves (L. Galiano et al., 2011; L. Galiano et al., 2012; Lloret et al., 2004), and increased likelihood of biotic attacks on stressed vegetation (Anderegg, Hicke, et al., 2015). Repeated droughts thus inhibit ecosystem recovery from individual drought events, accelerating changes in ecosystem composition, structure, and function (Fensham et al., 2009; Phillips et al., 2010). Site-level observations have reported increased mortality of dominant species, shifts in functional composition of ecosystems, and reduced above-ground biomass as a result of repeated or prolonged droughts (da Costa et al., 2010; Evans et al., 2011; Phillips et al., 2010). Regional-scale analyses have also indicated that repeated droughts could affect the global carbon cycle on decadal scales, largely offsetting the carbon sink of intact forests in non-drought years (Lewis et al., 2011). Legacy effects on tree growth rate have been observed well after drought cessation (Anderegg, Schwalm, et al., 2015; Kannenberg et al., 2020) and they could carry over into further drought periods, degrading tree health and even inducing mortality.

In addition, experiments involving land surface modeling demonstrated a decreasing trend in annual carbon storage along repeated exposure of intense droughts (Hoover & Rogers, 2016). Through comparing the effects of press-drought (chronic but moderate drought) and pulse-drought (short-term but extreme drought) as well as their interaction on mean annual total carbon anomaly, Hoover and Rogers (2016) suggest that interannual drought pattern may be as important as drought magnitude in affecting ecosystem carbon dynamics. However, due to lacking enough data, most process-based models are not well constrained, which introduces uncertainties and precludes useful prediction especially at large spatial-temporal scales (Adams et al., 2013; C. Xu et al., 2013).

Long-term observations provide an alternative approach to investigate vegetation response to recurrent droughts. Tree ring measurements and long-term flux tower observations have demonstrated great potential for examining drought responses at different timescales (e.g., Y. Liu et al., 2019; Serra-Maluquer et al., 2018), but site-level observations are limited in informing responses over large areas. The accumulation of remote sensing observations over the past three decades, on the other hand, enables investigation of vegetation responses to recurrent droughts at regional-to-continental scales. Through comparing the temporal dynamics of productivity and phenology metrics derived from the time series of normalized difference vegetation index for four different drought clusters, Ivits et al. (2014) found great bioclimatic difference among European ecosystems in response to recurrent droughts between 1992 and 2010. However, their analysis summarized vegetation responses over entire drought time series without distinguishing the contribution of the interannual drought pattern from overall drought impacts. Moreover, whilst the use of vegetation greenness indices to examine drought impact is commonplace, other biophysical variables that are directly associated with ecosystem structure and functions (e.g., vegetation fractional cover and canopy optical depth), have been seldom explored in response to recurrent drought events.

Between 1997 and 2009, Australia experienced a record-breaking, multi-year drought, known as the MD (Heberger, 2011). Examining the impacts of this drought provides a unique opportunity to explore the effect of recurrent droughts at a continental scale and may shed light on the impacts of long-lasting droughts in future hydroclimates. The objective of this study is to examine possible additional vegetation declines at same DI resulting from the temporal pattern of repeated droughts, hereafter called cumulative effects, over Australia during a

**Table 1**  
*Data Sources Used in This Study*

Data source	Parameter	Spatial	Temporal
		Resolution/Extent	Resolution/Extent
AVHRR-based product <sup>a</sup>	FPAR	0.01°, Australia	Monthly, 1992–2011
MODIS-based product 3.0.1 <sup>b</sup>	PVC	500 m, Australia	Monthly, 2000–2012
SSM/I, TMI, AMSR-1 fusion <sup>c</sup>	VOD	0.25°, Australia	Monthly, 1993–2012
ANUclimate 1.0 <sup>d</sup>	Precipitation (mm)	0.01°, Australia	Monthly, 1970–2012
eMAST-R-Package 2.0 <sup>e</sup>	PET (mm)	0.01° Australia	Monthly, 1970–2012
MCD64A1.051 <sup>f</sup>	Burned area	500 m, Australia	Monthly, 2000–2012
AVHRR Fire Frequency <sup>g</sup>	Fire Frequency	0.01°, Australia	One image, 1997–2009
NVIS v5.0 <sup>h</sup>	Major Vegetation Groups	100 m, Australia	One image, 1997–2009

<sup>a</sup>(R. J. Donohue et al., 2013). <sup>b</sup>(Guerschman, 2014). <sup>c</sup>(T. Xu et al., 2016). <sup>d</sup>Y. Y. Liuet al., (2009). <sup>e</sup>(Hutchinson et al., 2016). <sup>f</sup>(Giglio et al., 2009; Paget & King, 2011). <sup>g</sup>(Craig et al., 2002). <sup>h</sup>(NVIS, 2018).

20-year period centered by the MD. Canopy variables derived from multiple remotely sensed data sources were used to indicate vegetation response, including fraction of absorbed photosynthetic active radiation (FPAR), photosynthetic vegetation cover (PVC), and canopy density (a transformed version of Vegetation Optical Depth (VOD) derived from passive microwave data). We quantified the frequency and magnitude of cumulative effects of droughts during uninterrupted dry periods in fire-free areas of Australia, addressing the following specific questions: (a) How prevalent were cumulative effects as quantified by FPAR, PVC, and canopy density? (b) Which bioclimatic setting was most likely to experience cumulative effects when exposed to repeated or long-duration drought? (c) Which bioclimatic setting demonstrated the largest magnitude of impact from cumulative effects?

## 2. Data and Methods

### 2.1. General Description

We quantified the occurrence and magnitude of cumulative effects in the drought response of FPAR, PVC, and VOD-derived canopy density from remote sensing (Table 1). All the RS-derived variables were analyzed at their original resolution and then summarized at a common bioclimatic scale. We performed the analysis at a pixel level for all of Australia, excluding pixels where more than 10% the area burned during the assessment period according to a fire mask generated by combining the fire frequency map derived from Advance Very High-Resolution Radiometer (AVHRR) and the images of the fraction of pixel area that was burned generated with observations from Moderate Resolution Imaging Spectroradiometer (MODIS). We analyzed how the frequency and magnitude of cumulative effects varied across land cover types and across aridity levels, using the combination of one-way analysis of variance and a post hoc analysis with Tukey's honest significant differences to identify significant differences among group means.

### 2.2. Data Sources

#### 2.2.1. Time Series of FPAR, PVC, and Canopy Density

Cumulative effects were quantified for three different spaceborne observations of ecosystem properties, including monthly datasets of AVHRR fraction of absorbed photosynthetic active radiation (FPAR, 1 km), MODIS photosynthetic vegetation cover (PVC, 500 m) data, and canopy density derived from vegetation optical depth (VOD, 25 km) based on passive microwave data (Table 1). Most of the datasets cover the entire MD period plus a few years before and after. To increase the number of drought series for examining cumulative effects, all available time series covering the MD period were included for analysis. Each data set is briefly described here, with additional details presented in Jiao et al. (2020).

FPAR refers to the fraction of incident photosynthetically active radiation (PAR, total radiation at wavelengths of 400–700 nm) intercepted by green canopies. It can be regarded as a radiometric surrogate of leaf area index

in terrestrial vegetation (Running et al., 2000) which is closely related to surface energy and water fluxes (Asrar et al., 1984) as well as the net primary production (Monteith, 1981). A monthly AVHRR-based FPAR product obtained from Commonwealth Scientific and Industrial Research Organization (CSIRO) Land and Water Research was used to assess the dynamics of leaf area and PAR absorption in response to the MD spanning the Australian continent. Issues of orbital drift and time series data stretching across different satellites were addressed with a calibration procedure described in Donohue (R. J. Donohue et al., 2009).

PVC indicates the exposed proportion of Photosynthetic Vegetation (PV) within an instantaneous field of view (IFOV) of a remote sensing imaging system, which, in combination with Non-Photosynthetic Vegetation and Bare Soil, is assumed to compose the scene of an IFOV. A monthly PVC data set derived from a linear unmixing methodology (Guerschman et al., 2015) with all 7 MODIS bands was used to quantify the variation of spatial coverage of PV in response to drought.

Canopy density represents canopy structure and water content derived from a measure of canopy transmissivity derived from VOD, which itself is measured with passive microwave imaging or radiometers. (Y. Y. Liu et al. (2011)). The monthly VOD product used in this paper is retrieved from brightness temperatures of microwave data compiled across several sensor platforms with the use of a Land Parameter Retrieval Model (Owe et al., 2001, 2008). A more detailed description of the VOD product and associated canopy density can be found in Section 2.2.1 of Jiao et al. (2020).

### 2.2.2. Fire Mask

Fire is prevalent across Australia and strongly influences vegetation cover and composition (Maier, 2010). We used the MODIS burned area product combined with AVHRR fire history map (Table 1) to identify areas that experienced fires since 1997. Due to the difference in spatial resolution between MODIS and AVHRR fire products, a combined fire mask was first generated at a fine resolution, that is, 500 m. We then used the 500-m fire mask to calculate burn fraction for the spatial grid of each vegetation variable. This study excluded pixels with more than 10% burned areas from 1997 to 2011 or 2012, depending on the end of variable time series analyzed.

### 2.2.3. Ancillary Maps

A biome map and wet index map were adopted to analyze cumulative effects among bioclimatic settings. Biome assignments for each pixel were obtained from a reclassification of the 32 major vegetation groups in Australian National Vegetation Information System (NVIS, v5.0) into seven land-cover types, that is, *non-vegetation*, *other vegetation*, *cultivated lands*, *herbaceous*, *shrubs*, *savannas*, and *forests* (Figure S7 in Supporting Information S1). Only five land-cover types were examined in this study, namely cultivated lands, herbaceous, shrubs, savannas, and forests. A wetness index map was generated from the ratio of mean annual precipitation to mean annual potential evapotranspiration, which was then classified into five levels of aridity according to the standard of the United Nations Environment Program (1992). Each vegetation variable has a biome map and an aridity level map generated at its spatial resolution. The biome map was created by resampling biome types at the spatial grid of a vegetation variable assigning the majority class. The aridity level map was generated by resampling related climatic properties (e.g., mean annual precipitation and evapotranspiration) at a given resolution first using the method of average (fine to coarse) or nearest neighbor (coarse to fine), then calculating the wetness index, and lastly reclassifying the index into five levels.

## 2.3. Drought Intensity and Definition

We characterized DI on a pixel-by-pixel basis with absolute and standardized climatological water balance (WB) anomalies as follows. The climatological WB was calculated as the difference between precipitation (P) and potential evapotranspiration (PET) that was estimated using the Priestley-Taylor Method (see Equation 22 in Davis et al. (2017)) with inputs of mean monthly total daily shortwave radiation and mean monthly daily mean air temperature from the ANUCLIM products (Hutchinson et al., 2014) generated from observed Bureau of Meteorology data (Table 1). The Priestley-Taylor Method estimates potential evapotranspiration over saturated land surface using an empirical coefficient times the water-equivalence of net surface radiation, ignoring the soil heat flux (Lhomme, 1997; Priestley & Taylor, 1972). To consider the effect of soil water storage on plant water availability, both absolute and standardized DI indicators can be calculated at multiple time scales. In this paper, the 6-month time scale was analyzed, as the average length of water memory in vegetation productivity

is approximately 5.6 months in arid and semi-arid regions like Australia (L Liu et al., 2018). Thus, WB for a given month is the difference between the sums of P and PET over the 6 months up to and including that month. We computed each month's absolute WB anomaly (WBA) as the departure of monthly WB from the long-term (1970–2012) mean for that calendar month:

$$WBA_{y,m} = WB_{y,m} - \overline{WB}_{1970-2012,m} \quad (1)$$

where  $y$  and  $m$  indicate a given year and month respectively, and 1970–2012 refers to the period from the year of 1970 to the year of 2012.

We also computed a standardized water balance anomaly (SWBA) as the ratio between WBA and a pixel's standard deviation of WB for that calendar month:

$$SWBA_{y,m} = WBA_{y,m} / SD(WB_m) \quad (2)$$

Absolute and standardized representations offer two different perspectives on hydrologic anomalies, with the former measuring DI in unit of millimeter (Figure S1b in Supporting Information S1) and the latter allowing DI to be compared across aridity levels (Figure S1a in Supporting Information S1). At site level, SWBA shows consistent temporal variation with standardized precipitation evapotranspiration index (Vicente-Serrano et al., 2010), a metric commonly used in drought assessments. In addition, our drought indicators allow a comprehensive assessment of DI by providing a relative metric that is comparable over time and space and simultaneously informing the exact amount of water deficit in a interpretable unit (millimeter).

A drought event was defined as a period in which the WB was one standard deviation below its long-term mean for a given month, assuming that climatic WB is normally distributed:

$$Drought_{y,m} = \begin{cases} 1 \text{ (drought), } SWBA_{y,m} < -1 \\ 0 \text{ (non - drought), otherwise} \end{cases} \quad (3)$$

We examined cumulative effects by comparing drought events during an uninterrupted dry period, defined as a period in which  $SWBA < 1$  for all months.

All drought indicators were calculated at the spatial resolution of each vegetation variable. First, we calculated the monthly WB at a 6-month time scale at the resolution of climatic variables (P or PET). Second, the monthly WB were resampled at the spatial grid of each vegetation variable using the method of average (fine to coarse) or nearest neighbor (coarse to fine). Third, based on resampled monthly WB, we calculated absolute and standardized DI, and identified drought events along the time series of standardized DI.

#### 2.4. Identification and Quantification of Cumulative Effects

Cumulative effects (CE) refer to the non-linear increases in vegetation declines at same DI resulting from the temporal pattern of repeated droughts. They are identified as present for a given uninterrupted dry period if at least one growing season month is found to have an across-year positive trend in drought sensitivity for a vegetation variable (Equation 4, Figure 1). That is, a cumulative effect occurred if dry to normal conditions persisted for more than 2 years, and the drought sensitivity for a given growing season month increased in later years. Our analysis excluded dry periods with wet events ( $SWBA > 1$ ) in between drought events because we'd like to focus on ecosystem resistance and minimize the influence of wet events in the identification of cumulative effects. It has been implied that wet events could limit the ability of detecting the compound effects of repeated droughts in forests of the Amazon (Feldpausch et al., 2016). We assumed that wet events are likely to allow vegetation to reach full recovery before being exposed to following drought conditions. It is thus less likely to detect the cumulative effects when drought series are interrupted by wet periods. We used an increase in drought sensitivity over time to identify cumulative effects because both theoretical prediction and field observations show that ecosystems tend to lose their resistance and resilience to recurrent stressful events (Scheffer et al., 2001; Serra-Maluquer et al., 2018). To be precise:

$$CE(ds) = \begin{cases} 1 \text{ (yes), at least one } m \text{ with significant positive temporal trend in } S_{y,m}^{\text{absolute}} \\ 0 \text{ (no), Otherwise} \end{cases} \quad (4)$$

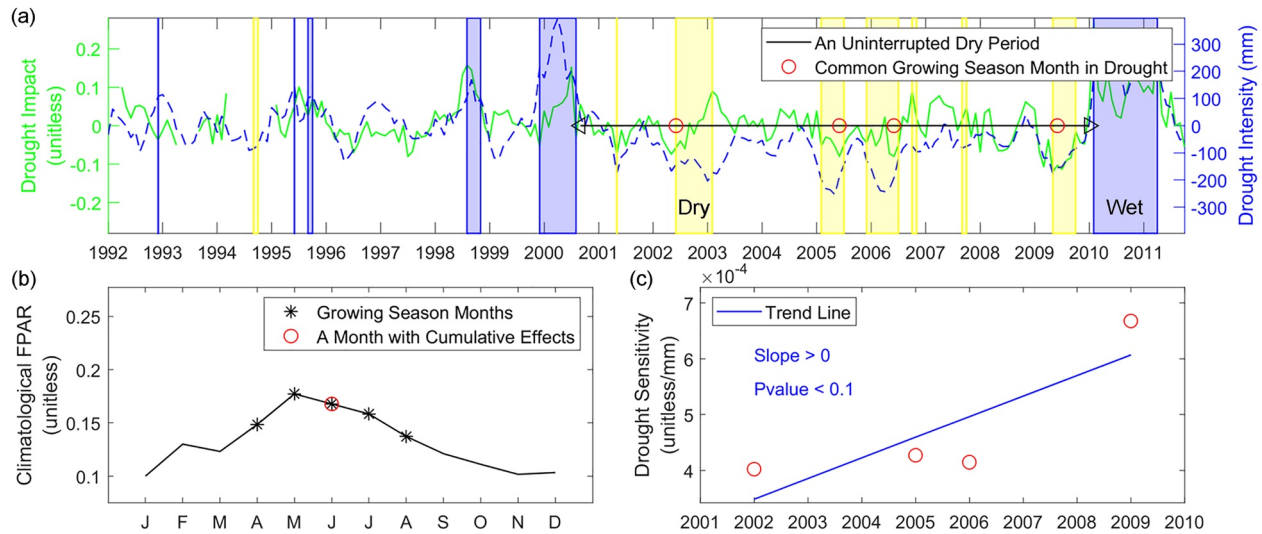


**Figure 1.** Identification of cumulative effects with three steps. (a) Identifying an uninterrupted dry period and a common growing season month in drought, in which yellow backgrounds indicate periods in drought, standardized water balance anomaly  $< -1$ , while blue backgrounds indicate wet events,  $SWBA > 1$ ; (b) Growing season months identified with climatological FPARs; (c) Significant increasing trend ( $P$ -value  $< 0.1$ ) in drought sensitivities across years. The data used is extracted from a typical pixel at the resolution of canopy density. The time traces in panel (a) indicated drought intensity (blue dashed line) and drought impact on FPAR (green solid line).

where  $ds$  refers to an uninterrupted dry period, that is, a time period with dry-to-normal hydrological conditions ( $SWBA < 1$ ) and having at least one common month in drought for 3 years or more;  $m$  refers to a month in the growing season, which is identified as the 5 months with the highest climatological FPAR; and  $S_{y,m}^{absolute}$  refers to absolute drought sensitivity, which is measured as the absolute departure of a variable ( $V_{y,m}$ ) from its baseline ( $V_{y,m}^{baseline}$ ) per unit change in WB anomaly (unit per mm).

$$S_{y,m}^{absolute} = (V_{y,m} - V_{y,m}^{baseline}) / WBA_{y,m} \quad (5)$$

Baseline conditions were defined by a normal WB, meaning when the  $SWBA$  was within the range  $(-1, 1)$ , in the same season and within a 6-year window centered on a given month. Only  $S_{y,m}^{absolute}$  with positive values were included in the analysis because negative or zero values imply that the vegetation is not sensitive to drought, making it difficult to physically interpret results. Since few samples (usually 3 or 4) were available for trend analysis in an uninterrupted dry period, positive slopes with  $P$ -value less than 0.1 were regarded as significant positive temporal trends. As such, the frequency of cumulative effects was based on the number of uninterrupted dry periods and quantified as the probability of uninterrupted drought periods showing cumulative effects. The number of growing season months with CE was recorded for each uninterrupted dry period as well. We deliberately restricted analysis to assessing positive slopes (rising impacts for successive drought events) ignoring possible negative slopes that would indicated declining drought impact so that we highlight adverse or negative impacts that might be increasing with successive drought events. However, we acknowledge that negative slopes are certainly possible in cases with strong physiological or morphological adaptations to drought.

We quantified cumulative effects by differencing the drought impacts that were measured in raw absolute terms (ADI with CE as shown with Equation 6) from the expected drought impacts that would have occurred if there had not been an increase in drought sensitivity (ADI without CE as shown with Equation 7).

$$ADI_{ds}^{with CE} = S_{y,m,ds}^{absolute} * WBA_{y,m,ds} \quad (6)$$

$$ADI_{ds}^{without CE} = Detrended(S_{y,m,ds}^{absolute}) * WBA_{y,m,ds}. \quad (7)$$

The corresponding magnitude of cumulative effects is computed in both absolute ( $M$ ) and fractional relative ( $F$ ) terms, as follows, and averaged across uninterrupted dry periods that contained cumulative effects:

$$M_{ds}^{CE} = ADI_{ds}^{with CE} - ADI_{ds}^{without CE} \quad (8)$$

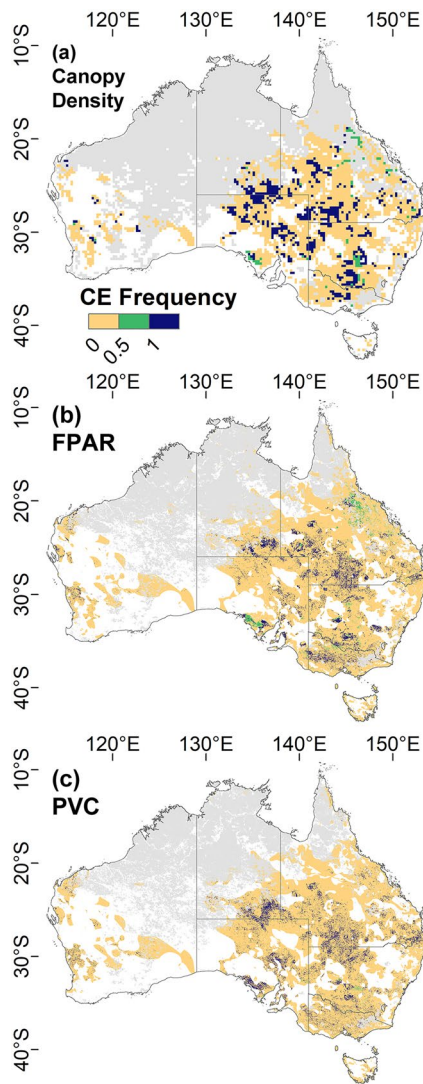


**Figure 2.** The frequency of cumulative effects quantified with Canopy Density (a), FPAR (b), and photosynthetic vegetation cover (c). Light gray indicates burn fraction >10%. White areas indicate no uninterrupted dry periods from 1992 to 2012. The frequency of cumulative effects was calculated as the ratio between the number of uninterrupted dry periods identified with cumulative effects and the total number of uninterrupted dry periods. The category with value “0” indicates no cumulative effects for extended dry periods, value “0.5” indicates that 50% of extended dry periods showed cumulative effects, and value “1” indicates that every uninterrupted dry period demonstrated cumulative effects.

frequency of cumulative effects for FPAR but not for canopy density and PVC. A similar biome pattern was found in the spatial coverage of cumulative effects over areas with recurrent drought (Table 2). Across aridity levels, more arid regions were more likely to show cumulative effects (Figure 4b).

In contrast, the magnitude of cumulative effects for bioclimatic regions showed a different pattern across bioclimatic regions. Among natural biome types, forests and savannas tended to have a larger fraction of drought impacts attributed to the repeated or long-duration drought pattern while shrublands experienced the smallest influence from CE (Figures 5a and 5c). Cultivated lands showed the highest absolute decline from CE for all canopy variables (Figure 5c) due to their rapid increases in drought sensitivity in successive droughts (Figure S5a in Supporting Information S1). Whereas the frequency of cumulative effects was shown to be higher in more arid

$$F_{ds}^{CE} = \frac{ADI_{ds}^{with\ CE} - ADI_{ds}^{without\ CE}}{ADI_{ds}^{with\ CE}} \quad (9)$$

### 3. Results

#### 3.1. The Frequency of Cumulative Effects

Canopy density, FPAR, and PVC tended to show consistent spatial patterns in the frequency of cumulative effects, with pixels showing higher frequencies scattered over the whole continent (Figure 2). The frequency of cumulative effects here shows three unique values that are 0, 0.5, and 1, as the total number of uninterrupted dry periods for CE identification is often limited to 1 or 2 during the period from the year 1992–2012 (Figure S2 in Supporting Information S1). Although more than 50% of fire-free areas experienced uninterrupted drought events (Table S1 in Supporting Information S1), less than 20% of these areas demonstrated cumulative effects in the response of canopy density, with even smaller extents for FPAR and PVC (less than 10%) (Table 2). The low spatial extent for all canopy variables indicates that cumulative effects are not prevalent over Australia during the MD period, implying the potential widespread existence of vegetation acclimation to drought conditions.

#### 3.2. The Magnitude of Cumulative Effects

Within the areas where we detected cumulative effects (8%–20% of the landscape), on average about 50% of the total drought impact was estimated to be induced by cumulative effects (Figure 3a–3c). The average magnitude of cumulative effects has uncertainty smaller than 3%, which applies to all biophysical variables. Corresponding absolute drought impacts were generally small, with around  $-0.07$  for FPAR,  $-0.04$  for PVC, and  $-0.03$  for canopy density (Figures 3d–3f), each referring to an absolute reduction in the variable in its raw units. Excluding cultivated lands does not change the overall distribution of magnitude of cumulative effects (Figure S3 in Supporting Information S1), differences in means in Table S2 in Supporting Information S1), implying that the impact of recurrent droughts was similar between human-managed and natural ecosystems. Also, spatial patterns were similar across the three biophysical variables, both for the fractional (Figures S4a–S4c in Supporting Information S1) and the absolute (Figures S4d–S4f in Supporting Information S1) magnitude of cumulative effects.

#### 3.3. Bioclimatic Differences

When exposed to long-term or repeated drought events, forests tended to have the lowest frequency of cumulative effects while grasslands had a relatively higher frequency of CE (Figure 4a). Cultivated lands had the highest



**Table 2**  
*Spatial Coverage of Cumulative Effects Over Areas With Uninterrupted Dry Periods*

Variable [time scale <sup>a</sup> ]	Canopy density [6M]			FPAR [6M]			PVC [6M]		
	Area with Uninterrupted Dry Periods (%) <sup>b</sup>	Area with CE (%) <sup>b</sup>	Percentage <sup>c</sup>	Area with Uninterrupted Dry Periods (%) <sup>b</sup>	Area with CE (%) <sup>b</sup>	Percentage <sup>c</sup>	Area with Uninterrupted Dry Periods (%) <sup>b</sup>	Area with CE (%) <sup>b</sup>	Percentage <sup>c</sup>
Forests	0.66	0.06	8.45%	1.91	0.10	5.15%	1.86	0.10	5.34%
Savannas	7.85	1.52	19.32%	10.68	0.92	8.59%	9.98	0.77	7.70%
Shrublands	7.08	1.63	22.98%	8.17	0.57	7.02%	7.92	0.63	7.96%
Grasslands	6.20	1.44	23.28%	7.42	0.74	9.96%	7.36	0.67	9.06%
Cultivated lands	8.02	1.29	16.15%	9.30	1.04	11.18%	8.47	0.74	8.68%
Total	29.81	5.94	19.92	37.49	3.37	8.99%	35.59	2.90	8.15%

<sup>a</sup>Time Scale refers to the time period of preceding water balance used in calculating current drought intensity. *M* indicates months. <sup>b</sup>Area (%) here is represented with the percentage of pixels in certain category relative to total land pixels of Australia at the spatial resolution of a vegetation variable. <sup>c</sup>Percentage indicates the spatial coverage of areas with CE over areas with at least one uninterrupted dry period from 1992 to 2012.

areas, the magnitude of cumulative effects tended to be larger in more humid regions (Figures 5b and 5d). Unlike cultivated lands, for which additional vegetation declines due to CE were mainly determined by an increase in drought sensitivity, the additional declines for natural ecosystems tended to be scaled by both the temporal variation in drought sensitivity as well as average DI. This could be found in the comparison across aridity levels in which only natural biomes were included. Compared to semi-arid regions which had the largest increase in

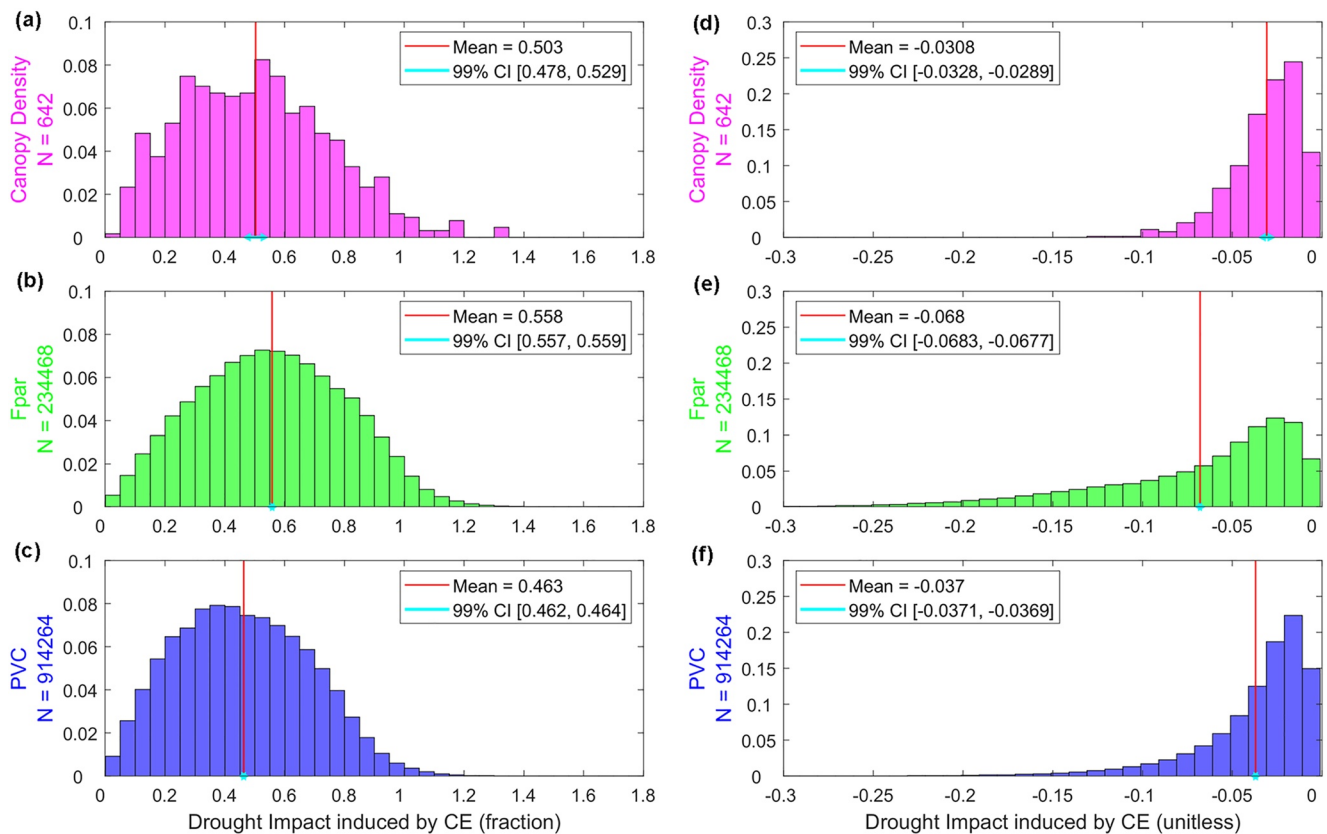


**Figure 3.** The histogram of the magnitude of cumulative effects (CE) with all biome types included. The left panel shows the fraction of total drought impact induced by CE (a–c) while the right panel shows associated absolute decline in the unit of canopy density (d), FPAR (e), and photosynthetic vegetation cover (f). *N* indicates the sample size of each canopy variables and the y axis corresponding to the probability of CE induced drought impacts which equals to the frequency normalized by sample size. 99% CI is short for 99% confidence interval for sample mean, which was estimated with 10,000 bootstraps.

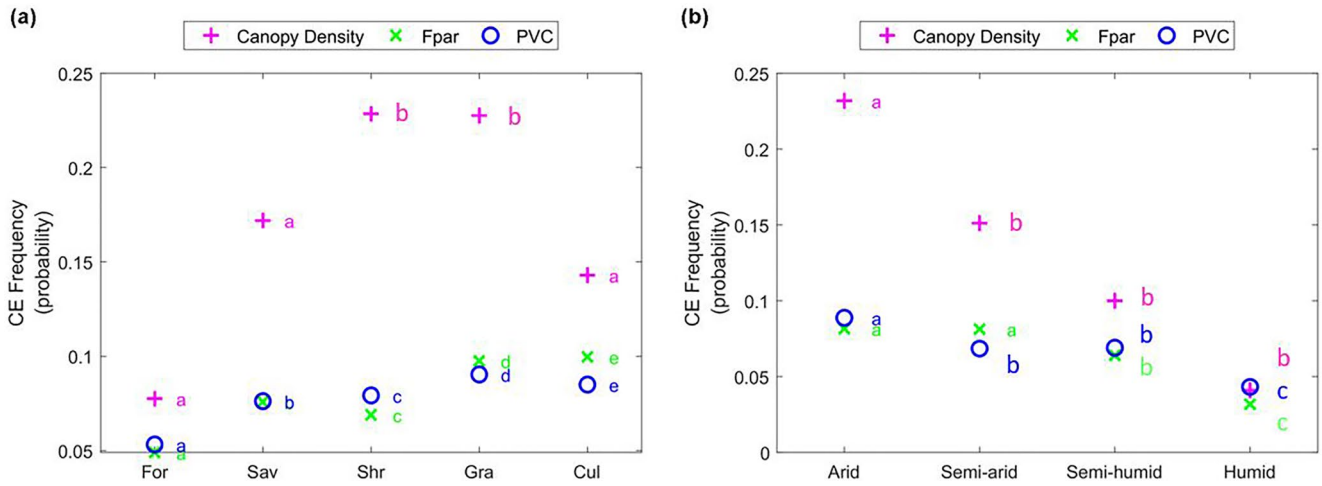


**Figure 4.** Comparison of the frequency of cumulative effects across (a) biome types, and (b) aridity levels. Markers sharing the same letter have mean values that are not significantly different. Cultivated lands are excluded from the analysis across aridity levels.

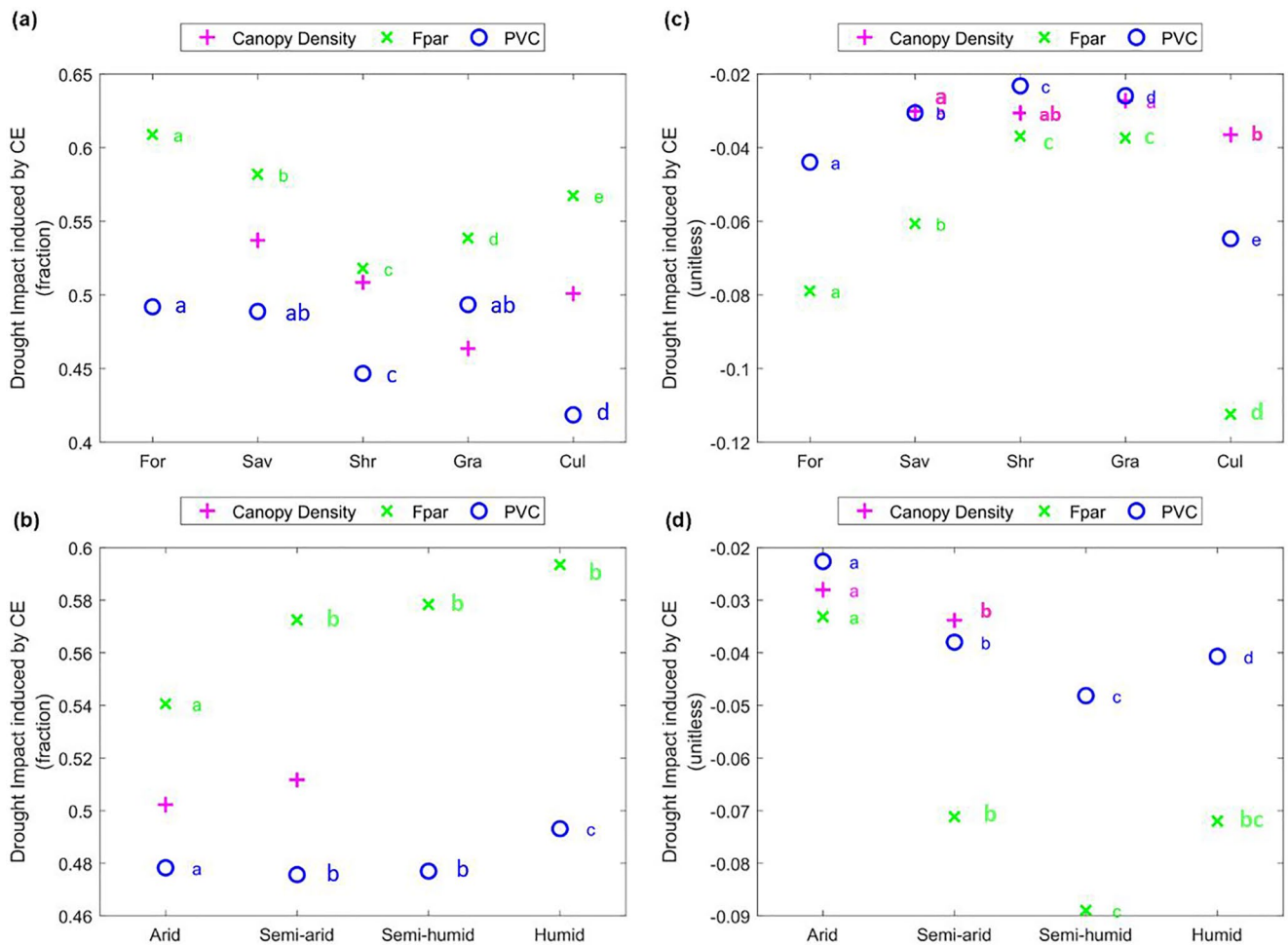


**Figure 5.** Comparison of the magnitude of cumulative effects in fractional and absolute metrics across (a, b) biome types, and (c, d) aridity levels. Groups with a sample size of less than 10 were excluded from the analysis. Markers sharing the same letter have mean values that are not significantly different. Cultivated lands are excluded from the analysis across aridity levels.

sensitivity (Figure S5b in Supporting Information S1), higher absolute decline in semi-humid regions (Figure 5d) were related to high DI (Figure S6b in Supporting Information S1). Meanwhile, in humid areas, high average DI did not result in greater decline than semi-humid regions, indicating that variation in sensitivity with recurrent droughts continued to be important in determining the magnitude of absolute decline.

## 4. Discussion

### 4.1. Summary of Findings

The MD, a decades-long drought across southeastern Australia, has previously been characterized as one continuous event, with dry years interspersed with average years (e.g., Ma et al., 2015). Here we examined this framing in more detail by characterizing the cumulative effects of drought during a period centered on the MD, finding that cumulative effects were not all that common. Although over 50% of fire-free areas were exposed to long-duration droughts of 3 years or longer without interruption, less than 20% of the exposed areas showed an increase in drought sensitivity. The limited occurrence of cumulative effects among all biomes indicates that most species over Australia are resistant to recurrent droughts. It could be explained by the prevalence of drought-tolerant species which adopt a conservative strategy in water usage and are thus insensitive to water deficit (Ouedraogo et al., 2013). Other plant adaptations that contribute to drought resistance include dehydration avoidance and summer dormancy, both of which involve changes in physiological processes (Backhaus et al., 2014; Boyko & Kovalchuk, 2011; Bruce et al., 2007) and morphological traits during severe drought (Bolger et al., 2005; Volaire et al., 2009). Besides these survival strategies, an absence of rising sensitivity to repeated droughts could also result from die-off from a first drought event followed by incomplete recovery. However, in the areas where cumulative effects (CE) were detected, about half of the total drought impact was attributed to the increasing trend of drought sensitivity induced by successive droughts.

Among biome types, forests and savannas tended to have relatively low frequency of cumulative effects but higher magnitude of CE. This could result from the deeper rooting of trees that provides access to additional water resources (e.g., Duursma et al., 2011) and thus reduces the response to successive droughts. Also, it could be related to saturation of vegetation indices (FPAR and PVC) with increasing LAI that could potentially mask leaf area losses in ecosystems that have more leaf area. Even if woody vegetation types are less vulnerable, the resistance of trees could be threatened over longer periods of recurrent droughts (Saunier et al., 2018). Repeated drought exposure has been shown to facilitate tree-level morphological adjustment like reduced their overall leaf area and biomass (Pritzkow et al., 2021). It could even cause community-level structural shifts such as the replacement of large trees with short, multi-stemmed individuals (Matusick et al., 2016). Shrublands, by contrast, had higher frequency of CE but the lowest magnitude of CE. Due to the differences in physiology and rooting patterns, many shrubs are more drought tolerant than trees (Allen et al., 2015; McDowell et al., 2011), which allows them to be less affected by recurrent drought exposure. Recent studies have shown that shrubs are often adapted to withstand long-term drought conditions (Schwinning et al., 2004), and thus are likely to replace other life forms under future climate with drought extremes (Bestelmeyer et al., 2015; D. D. Breshears et al., 2016). In addition, the variation across aridity levels shows that more humid areas would be less likely affected by recurrent droughts but, once they were affected, they would have greater additional declines from the drought pattern. This is consistent with the variation of drought tolerance across aridity levels, with vegetation that proliferated in more arid regions more adapted to recurrent droughts. In contrast, vegetation in more humid regions are less adapted to droughts and thus will experience larger impacts of drought extremes.

Cultivated lands and grasslands are most vulnerable to the impact of long-term drought as they had both higher frequency and larger magnitude of cumulative effects. Although management practices like replanting or rotation of crops could confound the interpretation of the results of CE in croplands, such as with annual grain crops, we note that grains only account for about one third of the agricultural land uses in Australia based on the investigation of 2005/2006 (Marinoni et al., 2012). Livestock and dairy productions are the dominant land uses of cultivated lands, making them similar in response to recurrent droughts as the grasslands.

### 4.2. Improved Understanding Through Synthesizing Distinct Canopy Variables

FPAR, PVC, and canopy density demonstrated consistent variation across bioclimatic settings in terms of the spatial coverage, the frequency and the magnitude of cumulative effects. Relatively high spatial coverage and

frequency of cumulative effects were detected for canopy density compared to FPAR and PVC. This could be partially attributed to their differing spatial resolutions, with canopy density at a pixel resolution of 25 km differing from FPAR (1 km) and PVC (0.5 km). In contrast, FPAR and PVC generally had larger cumulative effects than canopy density and their drought sensitivity increased faster along recurrent droughts, indicating that photosynthetic tissues were more vulnerable to uninterrupted interannual droughts than canopy biomass. Admittedly, satellite observations at the kilometer-scale resolution makes it difficult to decompose the change in drought sensitivity into the changes for woody or herbaceous components especially over heterogeneous surface like mixed woodlands. However, synthesizing results for distinct canopy variables advances our understanding about vegetation response to recurrent droughts ranging from radiative and structural properties to canopy biomass.

#### 4.3. Cumulative Effects Scaled by Both Elevated Sensitivity and Drought Intensity

Compared to the absolute decline induced by cumulative effects, the fractional impact provides a more effective way to estimate the contribution of interannual drought pattern because it expresses CE as a fraction of the total drought impact, accounting for variations with DI and other factors. We found that, when cumulative effects occur, they account for about 46 ~ 56% of the total drought impact for all vegetation types. This finding may allow us to estimate the overall impact of future recurrent droughts as a doubling of the impact induced by the first drought event in an uninterrupted dry period. At the same time, it is important to keep in mind that elevated sensitivity to drought due to prior drought exposure interacts with the DI of successive droughts, and the absolute impact can be moderated by a less intense follow-on drought. This complicates the assessment and interpretation of cumulative effects and calls for the study of how drought sensitivity interacts with DI in determining absolute decline.

#### 4.4. Implications for Modeling Vegetation Response to Recurrent Droughts

Our findings have several implications for the modeling of ecosystem drought-response dynamics. First, our results suggest that it is important to jointly consider an elevated drought sensitivity of vegetation greenness, canopy density, and vegetation fractional cover for successive drought events. Failing to do so may significantly underestimate drought-induced declines which may be apparent in one variable and not another. We note that it is unclear for how long drought sensitivity remains elevated, indicating a need for future study. Second, both the probability of cumulative effects and the absolute magnitude of their impact vary across bioclimatic settings. For example, forests and savannas are less likely to show cumulative effects but, once they are affected, they will have largest impacts in terms of carbon losses. In contrast, shrublands are more likely to be affected by cumulative effects but the impact is relatively small. Third, in the limited instances where they occurred, cumulative effects tended to account for about 50% of total drought impacts and the fractional contribution varied little among biome types. That is, once cumulative effects occurred, the impact of recurrent droughts could be estimated as doubled impacts of the first drought event given unchanged DI. Thus, the key to modeling vegetation response lies in determining when cumulative effects will occur. Possible determinants of this occurrence may include DI, drought duration, the duration of a post-drought interval, the hydrologic status of post-drought intervals, and the recovery status after individual drought events. All of these are worthy of future study.

#### 4.5. Limitations of Our Methodology

It is worth noting a few challenges in our method of identifying cumulative effects. First, through excluding areas with burned fraction >10%, we implicitly assume no connection between cumulative effects and fire. However, a positive relationship between drought and wildfire has been widely observed across the globe (Abatzoglou & Kolden, 2013; Abatzoglou et al., 2018; A. P. Williams et al., 2015) and drought-driven fires are becoming dominant in the current century as a result of climate change (Cary & Banks, 2000; Pausas & Fernández-Muñoz, 2012). It is possible that the close relationship between drought and fire explained why cumulative effects were not prevalent over fire-free regions. So, in future studies, it is necessary to examine local thresholds of burned fraction below which their relationship disappears. Second, this analysis of drought pattern is limited to analysis of dry periods free of intervening wet events (above normal wetness). An alternative analysis of drought pattern might also consider including wet extremes in between drought events, but doing so might need to account for variability in

the degree of response or recovery during intervening wet periods and this could become an additional source of variability that may confound the assessment. Third, lagged responses, including carryover effects of declines due to prior droughts into an ensuing drought response, may confound our interpretation regarding sensitivity. That is to say, what we interpret here as a rise in sensitivity to the current drought could actually be a delayed response to a prior drought that carries over into a follow-on event. As our drought sensitivity is calculated with vegetation declines regarded as a whole, it is difficult to distinguish the immediate response from the delayed response using our method. Thus, we are unable to provide insights on them individually. However, we could inform the trend of overall response along repeated or recurrent drought events through cumulative effects.

## 5. Conclusion

This study found that 8%–20% of the drought-affected and fire-free areas have evidence of additional declines of leaf abundance, canopy cover, and density due to cumulative effects from recurrent droughts, and that when they occur, cumulative effects can account for as much as half of total drought impact, which provides a convenient way to estimate the impact of recurrent droughts. Cumulative effects with repeat drought exposure had larger effects in forests and savannas, suggesting a greater risk of carbon release given repeated or long-duration drought. Overall, these findings support the notion that in many cases the impacts of multiple extreme events is often well captured with a simple stationary response to individual extreme events, with the need to consider sequence of events only in a small subset of cases.

## Data Availability Statement

Data sources used in this study could be accessed with references in Table 1. Data and codes used for this study could be obtained from <https://doi.org/10.5281/zenodo.5861281>.

## References

- Abatzoglou, J. T., & Kolden, C. A. (2013). Relationships between climate and macroscale area burned in the western United States. *International Journal of Wildland Fire*, 22(7), 1003–1020. <https://doi.org/10.1071/WF13019>
- Abatzoglou, J. T., Williams, A. P., Boschetti, L., Zubkova, M., & Kolden, C. A. (2018). Global patterns of interannual climate–fire relationships. *Global Change Biology*, 24(11), 5164–5175. <https://doi.org/10.1111/gcb.14405>
- Adams, H., Williams, A., Xu, C., Rauscher, S., Jiang, X., & McDowell, N. (2013). Empirical and process-based approaches to climate-induced forest mortality models. *Frontiers of Plant Science*, 4(438). <https://doi.org/10.3389/fpls.2013.00438>
- Allen, C. D., & Breshears, D. D. (1998). Drought-induced shift of a forest–woodland ecotone: Rapid landscape response to climate variation. *Proceedings of the National Academy of Sciences of the United States of America*, 95(25), 14839–14842. <https://doi.org/10.1073/pnas.95.25.14839>
- Allen, C. D., Breshears, D. D., & McDowell, N. G. (2015). On underestimation of global vulnerability to tree mortality and forest die-off from hotter drought in the Anthropocene. *Ecosphere*, 6(8), 1–55. <https://doi.org/10.1890/ES15-00203.1>
- Allen, C. D., Macalady, A. K., Chenchouni, H., Bachelet, D., McDowell, N., Vennetier, M., et al. (2010). A global overview of drought and heat-induced tree mortality reveals emerging climate change risks for forests. *Forest Ecology and Management*, 259(4), 660–684. <https://doi.org/10.1016/j.foreco.2009.09.001>
- Anderegg, W. R. L., Flint, A., Huang, C.-y., Flint, L., Berry, J. A., Davis, F. W., et al. (2015). Tree mortality predicted from drought-induced vascular damage. *Nature Geoscience*, 8(5), 367–371. <https://doi.org/10.1038/ngo2400>
- Anderegg, W. R. L., Hicke, J. A., Fisher, R. A., Allen, C. D., Aukema, J., Bentz, B., et al. (2015). Tree mortality from drought, insects, and their interactions in a changing climate. *New Phytologist*, 208(3), 674–683. <https://doi.org/10.1111/nph.13477>
- Anderegg, W. R. L., Kane, J. M., & Anderegg, L. D. L. (2013). Consequences of widespread tree mortality triggered by drought and temperature stress. *Nature Climate Change*, 3(1), 30–36. <https://doi.org/10.1038/nclimate1635>
- Anderegg, W. R. L., Plavcová, L., Anderegg, L. D., Hacke, U. G., Berry, J. A., & Field, C. B. (2013). Drought's legacy: Multiyear hydraulic deterioration underlies widespread aspen forest die-off and portends increased future risk. *Global Change Biology*, 19(4), 1188–1196. <https://doi.org/10.1111/gcb.12100>
- Anderegg, W. R. L., Schwalm, C., Biondi, F., Camarero, J. J., Koch, G., Litvak, M., et al. (2015). Pervasive drought legacies in forest ecosystems and their implications for carbon cycle models. *Science*, 349(6247), 528–532. <https://doi.org/10.1126/science.aab1833>
- Asrar, G. Q., Fuchs, M., Kanemasu, E. T., & Hatfield, J. L. (1984). Estimating absorbed photosynthetic radiation and leaf area index from spectral reflectance in wheat. *Agronomy Journal*, 76(2), 300–306. <https://doi.org/10.2134/agronj1984.00021962007600020029x>
- Backhaus, S., Kreyling, J., Grant, K., Beierkuhnlein, C., Walter, J., & Jentsch, A. (2014). Recurrent mild drought events increase resistance toward extreme drought stress. *Ecosystems*, 17(6), 1068–1081. <https://doi.org/10.1007/s10021-014-9781-5>
- Bestelmeyer, B. T., Okin, G. S., Duniway, M. C., Archer, S. R., Sayre, N. F., Williamson, J. C., & Herrick, J. E. (2015). Desertification, land use, and the transformation of global drylands. *Frontiers in Ecology and the Environment*, 13(1), 28–36. <https://doi.org/10.1890/140162>
- Bigler, C., Gavin, D. G., Gunning, C., & Veblen, T. T. (2007). Drought induces lagged tree mortality in a subalpine forest in the Rocky Mountains. *Oikos*, 116(12), 1983–1994. <https://doi.org/10.1111/j.2007.0030-1299.16034.x>
- Bolger, T. P., Rivelli, A. R., & Garden, D. L. (2005). Drought resistance of native and introduced perennial grasses of south-eastern Australia. *Australian Journal of Agricultural Research*, 56(11), 1261–1267. <https://doi.org/10.1071/AR05075>
- Boyko, A., & Kovalchuk, I. (2011). Genome instability and epigenetic modification—Heritable responses to environmental stress? *Current Opinion in Plant Biology*, 14(3), 260–266. <https://doi.org/10.1016/j.pbi.2011.03.003>

## Acknowledgments

This work was supported by NASA Headquarters under the NASA Earth and Space Science Fellowship Program (Grant 80NSSC17K0403 from 17-EARTH17F-0236).

- Breshears, D. D., Cobb, N. S., Rich, P. M., Price, K. P., Allen, C. D., Balice, R. G., et al. (2005). Regional vegetation die-off in response to global-change-type drought. *Proceedings of the National Academy of Sciences of the United States of America*, 102(42), 15144–15148. <https://doi.org/10.1073/pnas.0505734102>
- Breshears, D. D., Knapp, A. K., Law, D. J., Smith, M. D., Twidwell, D., & Wonkka, C. L. (2016). Rangeland responses to predicted increases in drought extremity. *Rangelands*, 38(4), 191–196. <https://doi.org/10.1016/j.rala.2016.06.009>
- Bruce, T. J. A., Matthes, M. C., Napier, J. A., & Pickett, J. A. (2007). Stressful “memories” of plants: Evidence and possible mechanisms. *Plant Science*, 173(6), 603–608. <https://doi.org/10.1016/j.plantsci.2007.09.002>
- Cary, G. J., & Banks, J. C. G. (2000). Fire regime sensitivity to global climate change: An Australian perspective. In J. L. Innes, M. Beniston, & M. M. Verstraete (Eds.), *Biomass burning and its inter-relationships with the climate system* (pp. 233–246). Springer Netherlands. [https://doi.org/10.1007/0-306-47959-1\\_13](https://doi.org/10.1007/0-306-47959-1_13)
- Ciais, P., Reichstein, M., Viovy, N., Granier, A., Ogee, J., Allard, V., et al. (2005). Europe-wide reduction in primary productivity caused by the heat and drought in 2003. *Nature*, 437(7058), 529–533. <https://doi.org/10.1038/nature03972>
- Craig, R., Heath, B., Raisbeck-Brown, N., Steber, M., Marsden, J., & Smith, R. (2002). *The distribution, extent and seasonality of large fires in Australia, April 1998–March 2000, as mapped from NOAA-AVHRR imagery* (pp. 1–77). Department of Land Administration.
- da Costa, A. C. L., Galbraith, D., Almeida, S., Portela, B. T. T., da Costa, M., de Athaydes Silva Junior, J., et al. (2010). Effect of 7 yr of experimental drought on vegetation dynamics and biomass storage of an eastern Amazonian rainforest. *New Phytologist*, 187(3), 579–591. <https://doi.org/10.1111/j.1469-8137.2010.03309.x>
- Dai, A. (2013). Increasing drought under global warming in observations and models. *Nature Climate Change*, 3(1), 52–58. <https://doi.org/10.1038/nclimate1633>
- Davis, T. W., Prentice, I. C., Stocker, B. D., Thomas, R. T., Whitley, R. J., Wang, H., et al. (2017). Simple process-led algorithms for simulating habitats (SPLASH v. 1.0): Robust indices of radiation, evapotranspiration and plant-available moisture. *Geoscientific Model Development*, 10(2), 689–708. <https://doi.org/10.5194/gmd-10-689-2017>
- Donohue, R. J., McVicar, T. R., & Roderick, M. L. (2009). Climate-related trends in Australian vegetation cover as inferred from satellite observations, 1981–2006. *Global Change Biology*, 15(4), 1025–1039. <https://doi.org/10.1111/j.1365-2486.2008.01746.x>
- Donohue, R. J., McVicar, T., & Roderick, M. (2013). Australian monthly IPAR derived from Advanced Very High Resolution Radiometer reflectances. <https://doi.org/10.4225/08/50FE0CBE0DD06>
- Doughty, C. E., Metcalfe, D., Girardin, C., Amézquita, F. F., Cabrera, D. G., Huasco, W. H., et al. (2015). Drought impact on forest carbon dynamics and fluxes in Amazonia. *Nature*, 519(7541), 78–82. <https://doi.org/10.1038/nature14213>
- Duursma, R. A., Barton, C. V. M., Eamus, D., Medlyn, B. E., Ellsworth, D. S., Forster, M. A., et al. (2011). Rooting depth explains [CO<sub>2</sub>] × drought interaction in Eucalyptus saligna. *Tree Physiology*, 31(9), 922–931. <https://doi.org/10.1093/treephys/tpr030>
- Evans, S. E., Byrne, K. M., Lauenroth, W. K., & Burke, I. C. (2011). Defining the limit to resistance in a drought-tolerant grassland: Long-term severe drought significantly reduces the dominant species and increases ruderals. *Journal of Ecology*, 99(6), 1500–1507. <https://doi.org/10.1111/j.1365-2745.2011.01864.x>
- Feldpausch, T. R., Phillips, O. L., Brienen, R. J. W., Gloor, E., Lloyd, J., Lopez-Gonzalez, G., et al. (2016). Amazon forest response to repeated droughts. *Global Biogeochemical Cycles*, 30(7), 964–982. <https://doi.org/10.1002/2015GB005133>
- Fensham, R. J., & Fairfax, R. J. (2007). Drought-related tree death of savanna eucalypts: Species susceptibility, soil conditions and root architecture. *Journal of Vegetation Science*, 18(1), 71–80. [https://doi.org/10.1658/1100-9233\(2007\)18\[1:DTDOSE\]2.0.CO;2](https://doi.org/10.1658/1100-9233(2007)18[1:DTDOSE]2.0.CO;2)
- Fensham, R. J., Fairfax, R. J., & Ward, D. P. (2009). Drought-induced tree death in savanna. *Global Change Biology*, 15(2), 380–387. <https://doi.org/10.1111/j.1365-2486.2008.01718.x>
- Floyd, M. L., Clifford, M., Cobb, N. S., Hanna, D., Delph, R., Ford, P., & Turner, D. (2009). Relationship of stand characteristics to drought-induced mortality in three Southwestern piñon–juniper woodlands. *Ecological Applications*, 19(5), 1223–1230. <https://doi.org/10.1890/08-1265.1>
- Galiano, L., Martínez-Vilalta, J., & Lloret, F. (2011). Carbon reserves and canopy defoliation determine the recovery of Scots pine 4 yr after a drought episode. *New Phytologist*, 190(3), 750–759. <https://doi.org/10.1111/j.1469-8137.2010.03628.x>
- Galiano, L., Martínez-Vilalta, J., Sabaté, S., & Lloret, F. (2012). Determinants of drought effects on crown condition and their relationship with depletion of carbon reserves in a Mediterranean holm oak forest. *Tree Physiology*, 32(4), 478–489. <https://doi.org/10.1093/treephys/tps025>
- Giglio, L., Loboda, T., Roy, D. P., Quayle, B., & Justice, C. O. (2009). An active-fire based burned area mapping algorithm for the MODIS sensor. *Remote Sensing of Environment*, 113(2), 408–420. <https://doi.org/10.1016/j.rse.2008.10.006>
- Guerschman, J. P. (2014). Fractional cover—MODIS, CSIRO Land and Water algorithm, Australia and global coverage.
- Guerschman, J. P., Scarth, P. F., McVicar, T. R., Renzullo, L. J., Malthus, T. J., Stewart, J. B., et al. (2015). Assessing the effects of site heterogeneity and soil properties when unmixing photosynthetic vegetation, non-photosynthetic vegetation and bare soil fractions from Landsat and MODIS data. *Remote Sensing of Environment*, 161, 12–26. <https://doi.org/10.1016/j.rse.2015.01.021>
- Heberger, M. (2011). Australia's millennium drought: Impacts and responses. In P. H. Gleick (Ed.), *The world's water: The Biennial report on freshwater resources* (pp. 97–125). Island Press/Center for Resource Economics. [https://doi.org/10.5822/978-1-59726-228-6\\_5](https://doi.org/10.5822/978-1-59726-228-6_5)
- Held, I. M., & Soden, B. J. (2006). Robust responses of the hydrological cycle to global warming. *Journal of Climate*, 19(21), 5686–5699. <https://doi.org/10.1175/JCLI3990.1>
- Hoover, D. L., & Rogers, B. M. (2016). Not all droughts are created equal: The impacts of interannual drought pattern and magnitude on grassland carbon cycling. *Global Change Biology*, 22(5), 1809–1820. <https://doi.org/10.1111/gcb.13161>
- Hutchinson, M., Kesteven, J., & Xu, T. (2014). ANUClimate collection.
- Hutchinson, M., Kesteven, J., Xu, T., & Stein, J. (2016). *Potential evapotranspiration: eMAST-R-package 2.0, 0.01 degree*. Australian Coverage.
- Ivits, E., Horion, S., Fensholt, R., & Cherlet, M. (2014). Drought footprint on European ecosystems between 1999 and 2010 assessed by remotely sensed vegetation phenology and productivity. *Global Change Biology*, 20(2), 581–593. <https://doi.org/10.1111/gcb.12393>
- Jiao, T., Williams, C. A., Rogan, J., De Kauwe, M. G., & Medlyn, B. E. (2020). Drought impacts on Australian vegetation during the millennium drought measured with multisource spaceborne remote sensing. *Journal of Geophysical Research: Biogeosciences*, 125(2), e2019JG005145. <https://doi.org/10.1029/2019JG005145>
- Kannenbergh, S. A., Schwalm, C. R., & Anderegg, W. R. L. (2020). Ghosts of the past: How drought legacy effects shape forest functioning and carbon cycling. *Ecology Letters*, 23(5), 891–901. <https://doi.org/10.1111/ele.13485>
- Keith, H., Van Gorsel, E., Jacobsen, K. L., & Cleugh, H. A. (2012). Dynamics of carbon exchange in a Eucalyptus forest in response to interacting disturbance factors. *Agricultural and Forest Meteorology*, 153, 67–81. <https://doi.org/10.1016/j.agrformet.2011.07.019>
- Lewis, S. L., Brando, P. M., Phillips, O. L., van der Heijden, G. M. F., & Nepstad, D. (2011). The 2010 Amazon drought. *Science*, 331(6017), 554. <https://doi.org/10.1126/science.1200807>
- Lhomme, J. (1997). A theoretical basis for the Priestley-Taylor coefficient. *Boundary-Layer Meteorology*, 82(2), 179–191. <https://doi.org/10.1023/A:1000281114105>

- Lindner, M., Maroschek, M., Netherer, S., Kremer, A., Barbati, A., Garcia-Gonzalo, J., et al. (2010). Climate change impacts, adaptive capacity, and vulnerability of European forest ecosystems. *Forest Ecology and Management*, 259(4), 698–709. <https://doi.org/10.1016/j.foreco.2009.09.023>
- Liu, L., Zhang, Y., Wu, S., Li, S., & Qin, D. (2018). Water memory effects and their impacts on global vegetation productivity and resilience. *Scientific Reports*, 8(1), 2962. <https://doi.org/10.1038/s41598-018-21339-4>
- Liu, Y., Schwalm, C. R., Samuels-Crow, K. E., & Ogle, K. (2019). Ecological memory of daily carbon exchange across the globe and its importance in drylands. *Ecology Letters*, 22(11), 1806–1816. <https://doi.org/10.1111/ele.13363>
- Liu, Y., Zhou, Y., Ju, W., Wang, S., Wu, X., He, M., & Zhu, G. (2014). Impacts of droughts on carbon sequestration by China's terrestrial ecosystems from 2000 to 2011. *Biogeosciences*, 11(10), 2583–2599. <https://doi.org/10.5194/bg-11-2583-2014>
- Liu, Y. Y., de Jeu, R. A. M., McCabe, M. F., Evans, J. P., & van Dijk, A. I. J. M. (2011). Global long-term passive microwave satellite-based retrievals of vegetation optical depth. *Geophysical Research Letters*, 38(18), L18402. <https://doi.org/10.1029/2011GL048684>
- Liu, Y. Y., van Dijk, A. I. J. M., de Jeu, R. A. M., & Holmes, T. R. H. (2009). An analysis of spatiotemporal variations of soil and vegetation moisture from a 29-year satellite-derived data set over mainland Australia. *Water Resources Research*, 45(7), W07405. <https://doi.org/10.1029/2008WR007187>
- Lloret, F., Siscart, D., & Dalmases, C. (2004). Canopy recovery after drought dieback in holm-oak Mediterranean forests of Catalonia (NE Spain). *Global Change Biology*, 10(12), 2092–2099. <https://doi.org/10.1111/j.1365-2486.2004.00870.x>
- Ma, X., Huete, A., Moran, S., Ponce-Campos, G., & Eamus, D. (2015). Abrupt shifts in phenology and vegetation productivity under climate extremes. *Journal of Geophysical Research: Biogeosciences*, 120(10), 2036–2052. <https://doi.org/10.1002/2015JG003144>
- Maier, S. W. (2010). Changes in surface reflectance from wildfires on the Australian continent measured by MODIS. *International Journal of Remote Sensing*, 31(12), 3161–3176. <https://doi.org/10.1080/01431160903154408>
- Marinoni, O., Navarro Garcia, J., Marvanek, S., Prestwidge, D., Clifford, D., & Laredo, L. A. (2012). Development of a system to produce maps of agricultural profit on a continental scale: An example for Australia. *Agricultural Systems*, 105(1), 33–45. <https://doi.org/10.1016/j.agsy.2011.09.002>
- Matusick, G., Ruthrof, K. X., Brouwers, N. C., Dell, B., & Hardy, G. S. J. (2013). Sudden forest canopy collapse corresponding with extreme drought and heat in a mediterranean-type eucalypt forest in southwestern Australia. *European Journal of Forest Research*, 132(3), 497–510. <https://doi.org/10.1007/s10342-013-0690-5>
- Matusick, G., Ruthrof, K. X., Fontaine, J. B., & Hardy, G. E. S. J. (2016). Eucalyptus forest shows low structural resistance and resilience to climate change-type drought. *Journal of Vegetation Science*, 27(3), 493–503. <https://doi.org/10.1111/jvs.12378>
- McDowell, N. G., Beerling, D. J., Breshears, D. D., Fisher, R. A., Raffa, K. F., & Stitt, M. (2011). The interdependence of mechanisms underlying climate-driven vegetation mortality. *Trends in Ecology & Evolution*, 26(10), 523–532. <https://doi.org/10.1016/j.tree.2011.06.003>
- Monteith, J. L. (1981). Climatic variation and the growth of crops. *Quarterly Journal of the Royal Meteorological Society*, 107(454), 749–774. <https://doi.org/10.1002/qj.49710745402>
- Mueller, R. C., Scudder, C. M., Porter, M. E., Talbot Trotter, R., Gehring, C. A., & Whitham, T. G. (2005). Differential tree mortality in response to severe drought: Evidence for long-term vegetation shifts. *Journal of Ecology*, 93(6), 1085–1093. <https://doi.org/10.1111/j.1365-2745.2005.01042.x>
- Nepstad, D. C., Tohver, I. M., Ray, D., Moutinho, P., & Cardinot, G. (2007). Mortality of large trees and lianas following experimental drought in an Amazon forest. *Ecology*, 88(9), 2259–2269. <https://doi.org/10.1890/06-1046.1>
- NVIS. (2018). National vegetation information system V5.0 present major vegetation groups.
- Ouédraogo, D.-Y., Mortier, F., Gourlet-Fleury, S., Freycon, V., & Picard, N. (2013). Slow-growing species cope best with drought: Evidence from long-term measurements in a tropical semi-deciduous moist forest of central Africa. *Journal of Ecology*, 101(6), 1459–1470. <https://doi.org/10.1111/1365-2745.12165>
- Owe, M., de Jeu, R., & Holmes, T. (2008). Multisensor historical climatology of satellite-derived global land surface moisture. *Journal of Geophysical Research*, 113(F1), F01002. <https://doi.org/10.1029/2007JF000769>
- Owe, M., de Jeu, R., & Walker, J. (2001). A methodology for surface soil moisture and vegetation optical depth retrieval using the microwave polarization difference index. *IEEE Transactions on Geoscience and Remote Sensing*, 39(8), 1643–1654. <https://doi.org/10.1109/36.942542>
- Paget, M., & King, E. (2011). *Active-fire based burned area - MODIS*. University of Maryland MCD64A1 mosaic.
- Pausas, J. G., & Fernández-Muñoz, S. (2012). Fire regime changes in the Western Mediterranean basin: From fuel-limited to drought-driven fire regime. *Climatic Change*, 110(1), 215–226. <https://doi.org/10.1007/s10584-011-0060-6>
- Phillips, O. L., Aragão, L. E., Lewis, S. L., Fisher, J. B., Lloyd, J., López-González, G., et al. (2009). Drought sensitivity of the Amazon rainforest. *Science*, 323(5919), 1344–1347. <https://doi.org/10.1126/science.1164033>
- Phillips, O. L., Van der Heijden, G., Lewis, S. L., López-González, G., Aragão, L. E., Lloyd, J., et al. (2010). Drought–mortality relationships for tropical forests. *New Phytologist*, 187(3), 631–646. <https://doi.org/10.1111/j.1469-8137.2010.03359.x>
- Ponce-Campos, G. E., Moran, M. S., Huete, A., Zhang, Y., Bresloff, C., Huxman, T. E., et al. (2013). Ecosystem resilience despite large-scale altered hydroclimatic conditions. *Nature*, 494(7437), 349–352. <https://doi.org/10.1038/nature11836>
- Priestley, C., & Taylor, R. (1972). On the assessment of surface heat flux and evaporation using large-scale parameters. *Monthly Weather Review*, 100(2), 81–92. [https://doi.org/10.1175/1520-0493\(1972\)100<0081:OTAOSH>2.3.CO;2](https://doi.org/10.1175/1520-0493(1972)100<0081:OTAOSH>2.3.CO;2)
- Pritzkow, C., Szota, C., Williamson, V., & Arndt, S. K. (2021). Previous drought exposure leads to greater drought resistance in eucalypts through changes in morphology rather than physiology. *Tree Physiology*, 41(7), 1186–1198. <https://doi.org/10.1093/treephys/tpaa176>
- Reichstein, M., Ciais, P., Papale, D., Valentini, R., Running, S., Viovy, N., et al. (2007). Reduction of ecosystem productivity and respiration during the European summer 2003 climate anomaly: A joint flux tower, remote sensing and modelling analysis. *Global Change Biology*, 13(3), 634–651. <https://doi.org/10.1111/j.1365-2486.2006.01224.x>
- Running, S. W., Thornton, P. E., Nemani, R., & Glassy, J. M. (2000). Global terrestrial gross and net primary productivity from the Earth Observing System. In O. E. Sala, R. B. Jackson, H. A. Mooney, & R. W. Howarth (Eds.), *Methods in ecosystem science* (pp. 44–45). Springer. [https://doi.org/10.1007/978-1-4612-1224-9\\_4](https://doi.org/10.1007/978-1-4612-1224-9_4)
- Saunier, A., Ormeño, E., Havaux, M., Wortham, H., Ksas, B., Temime-Roussel, B., et al. (2018). Resistance of native oak to recurrent drought conditions simulating predicted climatic changes in the Mediterranean region. *Plant, Cell and Environment*, 41(10), 2299–2312. <https://doi.org/10.1111/pce.13331>
- Scheffer, M., Carpenter, S., Foley, J. A., Folke, C., & Walker, B. (2001). Catastrophic shifts in ecosystems. *Nature*, 413(6856), 591–596. <https://doi.org/10.1038/35098000>
- Schwalm, C. R., Williams, C. A., & Schaefer, K. (2011). Carbon consequences of global hydrologic change, 1948–2009. *Journal of Geophysical Research*, 116(G3), G03042. <https://doi.org/10.1029/2011JG001674>
- Schwalm, C. R., Williams, C. A., Schaefer, K., Arneth, A., Bonal, D., Buchmann, N., et al. (2010). Assimilation exceeds respiration sensitivity to drought: A FLUXNET synthesis. *Global Change Biology*, 16(2), 657–670. <https://doi.org/10.1111/j.1365-2486.2009.01991.x>

- Schwalm, C. R., Williams, C. A., Schaefer, K., Baldocchi, D., Black, T. A., Goldstein, A. H., et al. (2012). Reduction in carbon uptake during turn of the century drought in western North America. *Nature Geoscience*, 5(8), 551–556. <https://doi.org/10.1038/ngeo1529>
- Schwinning, S., Sala, O. E., Loik, M. E., & Ehleringer, J. R. (2004). Thresholds, memory, and seasonality: Understanding pulse dynamics in arid/semi-arid ecosystems. *Oecologia*, 141(2), 191–193. <https://doi.org/10.1007/s00442-004-1683-3>
- Serra-Maluquer, X., Mencuccini, M., & Martínez-Vilalta, J. (2018). Changes in tree resistance, recovery and resilience across three successive extreme droughts in the northeast Iberian Peninsula. *Oecologia*, 187(1), 343–354. <https://doi.org/10.1007/s00442-018-4118-2>
- Sheffield, J., & Wood, E. F. (2008). Projected changes in drought occurrence under future global warming from multi-model, multi-scenario, IPCC AR4 simulations. *Climate Dynamics*, 31(1), 79–105. <https://doi.org/10.1007/s00382-007-0340-z>
- Suarez, M. L., & Kitzberger, T. (2008). Recruitment patterns following a severe drought: Long-term compositional shifts in Patagonian forests. *Canadian Journal of Forest Research*, 38(12), 3002–3010. <https://doi.org/10.1139/X08-149>
- Ukkola, A. M., De Kauwe, M. G., Roderick, M. L., Abramowitz, G., & Pitman, A. J. (2020). Robust future changes in meteorological drought in CMIP6 projections despite uncertainty in precipitation. *Geophysical Research Letters*, 47(11), e2020GL087820. <https://doi.org/10.1029/2020gl087820>
- van Dijk, A. I. J. M., Beck, H. E., Crosbie, R. S., Jeu, R. A. M., Liu, Y. Y., Podger, G. M., et al. (2013). The Millennium Drought in southeast Australia (2001–2009): Natural and human causes and implications for water resources, ecosystems, economy, and society. *Water Resources Research*, 49(2), 1040–1057. <https://doi.org/10.1002/wrcr.20123>
- Vicente-Serrano, S. M., Beguería, S., & López-Moreno, J. I. (2010). A multiscalar drought index sensitive to global warming: The standardized precipitation evapotranspiration index. *Journal of Climate*, 23(7), 1696–1718. <https://doi.org/10.1175/2009JCL12909.1>
- Voltaire, F., Norton, M. R., & Lelièvre, F. (2009). Summer drought survival strategies and sustainability of perennial temperate forage grasses in Mediterranean areas. *Crop Science*, 49(6), 2386–2392. <https://doi.org/10.2135/cropsci2009.06.0317>
- Williams, A. P., Seager, R., Macalady, A. K., Berkelhammer, M., Crimmins, M. A., Swetnam, T. W., et al. (2015). Correlations between components of the water balance and burned area reveal new insights for predicting forest fire area in the southwest United States. *International Journal of Wildland Fire*, 24(1), 14–26. <https://doi.org/10.1071/WF14023>
- Williams, C. A. (2014). Heat and drought extremes likely to stress ecosystem productivity equally or more in a warmer, CO<sub>2</sub> rich future. *Environmental Research Letters*, 9(10), 101002. <https://doi.org/10.1088/1748-9326/9/10/101002>
- Williams, C. A., Gu, H., MacLean, R., Masek, J. G., & Collatz, G. J. (2016). Disturbance and the carbon balance of US forests: A quantitative review of impacts from harvests, fires, insects, and droughts. *Global and Planetary Change*, 143, 66–80. <https://doi.org/10.1016/j.gloplacha.2016.06.002>
- Williams, I. N., Torn, M. S., Riley, W. J., & Wehner, M. F. (2014). Impacts of climate extremes on gross primary production under global warming. *Environmental Research Letters*, 9(9), 094011. <https://doi.org/10.1088/1748-9326/9/9/094011>
- Xu, C., McDowell, N. G., Sevanto, S., & Fisher, R. A. (2013). Our limited ability to predict vegetation dynamics under water stress. *New Phytologist*, 200(2), 298–300. <https://doi.org/10.1111/nph.12450>
- Xu, T., Kesteven, J., & Hutchinson, M. (2016). *Monthly total precipitation: ANUclimate 1.0, 0.01 degree*. Australian Coverage.